THE JOURNAL OF BIOLOGICAL CHEMISTRY
Vol. 279, No. 29, Issue of July 16, pp. 30158–30167, 2004

Printed in U.S.A.

Definition of a Consensus DNA-binding Site for PecS, a Global Regulator of Virulence Gene Expression in *Erwinia chrysanthemi* and Identification of New Members of the PecS Regulon*

Received for publication, March 25, 2004
Published, JBC Papers in Press, May 12, 2004, DOI 10.1074/jbc.M403343200

Carine Rouanet‡, Sylvie Reverchon, Dmitry A. Rodionov§, and William Nasser¶

From the Unité de Microbiologie et Génétique CNRS-Institut National des Sciences Appliquées-Université Claude Bernard Lyon, Unité Mixte de Recherche 5122 Université Claude Bernard Lyon, 69622 Villeurbanne Cedex, France

In *Erwinia chrysanthemi*, production of pectic enzymes is modulated by a complex network involving several regulators. One of them, PecS, which belongs to the MarR family, also controls the synthesis of various other virulence factors, such as cellulases and indigoidine. Here, the PecS consensus-binding site is defined by combining a systematic evolution of ligands by an exponential enrichment approach and mutational analyses. The consensus consists of a 23-base pair palindromic-like sequence ($C_{-11}G_{-10}A_{-9}N_{-8}W_{-7}T_{-6}C_{-5}G_{-4}T_{-3}A_{-2}$)$T_{-1}A_0T_1$($T_2A_3C_4G_5A_6N_7N_8N_9C_{10}G_{11}$). Mutational experiments revealed that (*i*) the palindromic organization is required for the binding of PecS, (*ii*) the very conserved part of the consensus (−6 to 6) allows for a specific interaction with PecS, but the presence of the relatively degenerated bases located apart significantly increases PecS affinity, (*iii*) the four bases G_{-4}, A_{-2}, T_2, and C_4 are required for efficient binding of PecS, and (*iv*) the presence of several binding sites on the same promoter increases the affinity of PecS. This consensus is detected in the regions involved in PecS binding on the previously characterized target genes. This variable consensus is in agreement with the observation that the members of the MarR family are able to bind various DNA targets as dimers by means of a winged helix DNA-binding motif. Binding of PecS on a promoter region containing the defined consensus results in a repression of gene transcription *in vitro*. Preliminary scanning of the *E. chrysanthemi* genome sequence with the consensus revealed the presence of strong PecS-binding sites in the intergenic region between *fliE* and *fliFGHIJKLMNOPQR* which encode proteins involved in the biogenesis of flagellum. Accordingly, PecS directly represses *fliE* expression. Thus, PecS seems to control the synthesis of virulence factors required for the key steps of plant infection.

* This work was supported by grants from the Centre National de la Recherche Scientifique, from the Ministère Délégué à la Recherche et aux Nouvelles Technologies, and from Programme de Microbiologie 2003 (ACIM-2-17). The costs of publication of this article were defrayed in part by the payment of page charges. This article must therefore be hereby marked "*advertisement*" in accordance with 18 U.S.C. Section 1734 solely to indicate this fact.

‡ Present address: Mécanisme Moléculaire de la Pathogénie Bactérienne Unité, INSERM 629, Institut Pasteur de Lille, 1 Rue du Prof. Calmette, 59019 Lille Cedex, France.

§ Working visit to Unité de Microbiologie et Génétique CNRS-Institut National des Sciences Appliquées-Université Claude Bernard Lyon was supported by an exchange grant within the European Science Foundation Programme on Integrated Approaches for Functional Genomics. Present address: State Scientific Center GosNII Genetica, Moscow 117545, Russia.

¶ To whom correspondence should be addressed. Tel.: 33-4-7243-2695; Fax: 33-4-7243-1584; E-mail: William.nasser@insa-lyon.fr.

The enterobacteria *Erwinia chrysanthemi* and other soft-rot *Erwinia* species can infect a wide range of economically important crops causing soft-rot diseases. The pathogenic behavior of these bacteria is characterized by a rapid necrosis of parenchymatous tissues, mainly caused by pectic enzymes that degrade the middle lamellae and the primary cell wall (1). Nevertheless, plant colonization by pectinolytic *Erwinia* is a multifactorial process requiring numerous additional factors, including cellulases (2), iron assimilation (3), the Hrp system (4), exopolysaccharides (5), motility (6), and proteins involved in resistance against plant defense mechanisms (7–9). The precise roles of these virulence factors in the various stages of disease are often ill defined. However, it seems clear that appropriate regulation of gene expression is essential for a pathogen to adapt to a particular host environment.

In *E. chrysanthemi*, the production of pectic enzymes is modulated by a complex network involving several regulatory proteins (10–14). Among them is the PecS protein, a member of the MarR family of transcriptional regulators that are required for the adaptation of a variety of bacteria to different environments. This family includes MarR and EmrR (*Escherichia coli*), which control genes involved in multiple antibiotic resistance; RovA, which plays a role in the regulation of the invasion of mammalian cells by *Yersinia enterocolitica* and mediates regulation of invasin in response to environmental signals; HprR (*Bacillus subtilis*) required for hydrogen peroxide resistance as well as for the control of sporulation; MexR, which regulates multidrug efflux systems in *Pseudomonas aeruginosa*; and SlyA$_{St}$ (*Salmonella typhimurium*), which is required for resistance against oxidative damage and survival in macrophages (15–20). In *E. chrysanthemi*, PecS acts as a repressor on the production of the degradative enzymes, *i.e.* pectate lyases and cellulases (21), and up-regulates the synthesis of polygalacturonase enzymes (22, 23). Furthermore, *pecS* mutants produce an extracellular blue pigment called indigoidine, which is involved in the resistance to the products of oxidative burst, including hydrogen peroxide (24). Consistent with its involvement in the regulation of the synthesis of a large group of virulence factors, it has been shown that PecS plays a key role in the virulence of *E. chrysanthemi* (24). The signal to which PecS responds is not yet known.

Previous experiments carried out on 11 natural PecS target genes have suggested that PecS binds to DNA as a dimer and acts by means of a direct mechanism by interacting with the regulatory regions of the controlled genes (22–27). Despite these works, relatively little is known about how PecS regulates gene expression. For example, the operator site to which PecS binds to control gene transcription has not been identified, and it is not clear whether PecS directly modulates the RNA polymerase activity on the controlled gene promoters. The

present study is aimed at more fully understanding the nature of the molecular mechanisms used by PecS to direct the gene expression control. A PCR-based systematic evolution of ligands by an exponential enrichment (SELEX)[1] approach and site-directed mutagenesis experiments were used to identify the PecS-binding site consensus; database searches revealed new members of the PecS regulon. Moreover, we report the use of *in vitro* transcription and potassium permanganate footprinting to monitor the action of PecS on RNA polymerase activity.

EXPERIMENTAL PROCEDURES

Chemicals and Enzymes—Chemicals and enzymes used in this work were obtained from commercial sources.

Bacterial Strains, Plasmids, and Microbiological Methods—Bacterial strains used in this work were *E. coli* DH5α (F′ ϕ80*dlacZ* Δ(*lacZYA-argF*)*U169deoR recA1* and *A1 hsdR17* (r_{k-1}, m_{k+}) *phoA supE44* λ-*thi-1 gyrA96 relA1*/*F′ proAB*$^+$ *lacI*^{q}*ZΔM15 Tn10-Tc*) (Invitrogen) and *E. chrysanthemi* strain A350 (*lmrTc lacZ2*) and its *pecS* derivative, A1524 (*lmrTc lacZ2 pecS*::MudIIPR13) (laboratory collection). All strains were grown in Luria-Bertani medium (10 g/liter tryptone, 5 g/liter yeast extract, 5 g/liter NaCl) supplemented, when required, with antibiotics at the following concentration: 100 μg/ml of ampicillin and 50 μg/ml chloramphenicol. To test motility, equal quantities of bacteria were loaded into holes in 0.4% Luria-Bertani agar plates. Plates were checked between 12 and 24 h after inoculation. Motility was determined by measuring the diameter of the colony.

The plasmid pCR 2.1 (Invitrogen) was used for the cloning of the SELEX products. The constructs pSR1235 and pSR1802 are described by Praillet *et al.* (25, 26). The plasmids pN1908, pN1912, and pN1946 are described by Nasser *et al.* (22). The construct pSR1919 was generated by deleting the 1675-bp NruI/SmaI from pSR1802. For construction of pWN2965, the *celZ* promoter region (330-bp NruI/EcoRV) from pSR1919 was cloned in the EcoRV site of pBluescript^{ApR} (Stratagene). The plasmid pWN2969 was generated by cloning the *fliE* regulatory region (361 bp, −313 to +48, relative to the translation initiation codon ATG) in the vector pCR 2.1.

RNA Isolation and Primer Extension Analysis—RNA extraction and normalization, as well as primer extension experiments, were essentially performed as described previously (28). The primers used for specific detection of mRNA were 5′ end-labeled: celZ1, 5′-CTGGATTCT-TATCCAAATAAGAGAGCGG-3′, which anneals to *celZ* mRNA molecules at positions +4 to +31 (relative to the translation initiation codon ATG); fliEpext, 5′-CGTCGATACCCTGAATAGAC-3′, and PFliE1R, 5′-CGGTAATCTGCATCTGCTGC-3′, which anneal +3 to +22 and +29 to +48, respectively (relative to the *fliE* translation initiation codon ATG). The extension products were resolved on a 6% sequencing gel and visualized by autoradiography on Amersham MP film. The length of the transcripts was identified by using the corresponding dideoxy sequencing reactions as a reference.

Proteins—PecS was isolated as described previously (26). The *E. coli* RNA polymerase holoenzyme was purchased from Epicentre (Epicentre, Madison, WI).

Band-shift Assay—PpecS, $PpecS_L$, $PpecS_H$, and PfliE were PCR-amplified using pSR1235 or pWN2969 DNA as templates and the pairs of primers PecSBanID (5′-GTGCCAATCACCAGCATGG-3′) and PecS-BglIR (5′-GCACATCCATGTGCAGTTCTC-3′), PecSBanID and PecM-48R (5′-GACATTGAATATTTCTTTCCGG-3′), PecM-46D (5′-GATGT-TATTGACATACTAATTACG-3′) and PecSBglIR, PFliE1R and PFliE2D (5′-GCTGAACGATATGGGTAACG-3′), respectively. The primers PecS-BanID, PecM-46D, PecM-48R, and PecSBglIR are complementary to +147 to +166, −64 to −41, −39 to −18, and −183 to −163, respectively (relative to the *pecS* transcription initiation site); the primers PfliED2 and PfliE1R are complementary to −313 to −294 and +29 to +48, respectively (relative to the *fliE* translation initiation codon). The primers PecSBanID, PecM-48D, and PfliED2 were uniquely end-labeled using (γ-^{32}P)ATP (5000 Ci/mmol, Amersham Biosciences) and T4 polynucleotide kinase. The fragments obtained were purified after electrophoresis on agarose gel using the Qiagen quick extraction kit. The PcelZ, PpehX, PpehV, and PpehW DNA fragments were recovered from plasmids pSR1919, pN1908, pN1912, and pN1946, respectively. These DNA fragments were further end-labeled with (α-^{32}P)dCTP or (α-^{32}P)dATP (3000 Ci/mmol, Amersham Biosciences), and the Klenow fragment of DNA polymerase was then purified as described above. Band-shift assays were performed as described previously (26), and apparent dissociation constants (K_d) were determined as described earlier (29). The signals obtained were detected by autoradiography on Amersham MP film and quantified using ImageMaster TotalLab version 2.01 software (Amersham Biosciences).

Selection of the PecS-binding Site from Random DNA Sequences—The method for binding-site selection was adapted from Tuerk and Gold (30). The following oligonucleotides were synthesized: R76, 5′-CAGGT-CAGTTCAGCGGATCCTGTCGN_{26}GAGGCGAATTCAGTGCAACTGC-AGC-3′, where *N* indicates that either G, A, T, or C was inserted at that position; RC23, 5′-CAGGTCAGTTCAGCGGATCCTGTCGCGACTTCG-TATATTACGACGTCGGAGGCGAATTCAGTGCAACTGCAGC-3′; RC13, 5′-CAGGTCAGTTCAGCGGATCCTGTCGTCGTATATTACGAG-AGGCGAATTCAGTGCAACTGCAGC-3′; O-celZ, 5′-CAGGTCAGTTC-AGCGGATCCTGTCGTATTGAAAATTCCGAGAATGAATCTAGCATG-AGGCGAATTCAGTGCAACTGCAGC-3′; O-pecS, 5′-CAGGTCAGTTC-AGCGGATCCTGTCGCGTATGCGTATATTACGAAATCGGAGGCGA-ATTCAGTGCAACTGCAGC-3′ pR, 5′-CAGGTCAGTTCAGCGGATCC-TGTCG-3′; pF, 5′-GCTGCAGTTGCACTGAATTCGCCTC-3′. Double-stranded DNA fragments were generated by one round of PCR with 0.2 μM oligonucleotides R76, RC23, RC13, O-pecS, or O-celZ as a template and 1 μM oligonucleotide pF as a primer in 40 μl of reaction mixture containing 50 μM each dGTP, dATP, and dTTP, 4 μM dCTP, 20 μCi (α-^{32}P)dCTP (3000 Ci/mmol, Amersham Biosciences), and 5 units of Taq polymerase (Promega). The reaction mixture was heated at 94 °C for 1 min, annealed at 62 °C for 3 min, and extended at 72 °C for 9 min; then, cold dCTP was adjusted to 50 μM followed by an extending reaction for 10 min. The reaction products were purified on a Sephadex G-25 MicroSpin column (Amersham Biosciences) and electrophoresed on an 8% acrylamide gel using 0.5 × TBE (90 mM Tris, 64.6 mM boric acid, 2.5 mM EDTA, pH 8.3) as running buffer. The double-strand DNA fragments, detected after a 5-min exposure on autoradiographic film, were excised and eluted by an overnight incubation at 30 °C in 0.5 M ammonium acetate, 1 mM EDTA, and 0.1% SDS. DNA fragments contained in the elution were precipitated for 30 min at −20 °C in the presence of 40 μg of glycogen and 1 volume of isopropanol. Recovered pellets were then rinsed with 70% ethanol and resuspended at 4×10^4 counts/min/μl in water. A sample (2 μl) of the resulting mixture was used for band-shift assays. The PecS-DNA complexes were then excised and extracted as described above. All of the recovered DNA was amplified by PCR with 10 μM of each primer pF and pR in 20 μl of mixture as described above. The reaction mixture was heated at 94 °C for 2 min; then, for each of 12 cycles, it was denatured at 94 °C for 1 min, annealed at 62 °C for 1 min, and extended at 72 °C for 1 min. The reaction products were purified on a Sephadex G-25 MicroSpin column and used for the next step of selection. After a total of seven rounds of selection and amplification, the eluted DNA was cloned into a pCR 2.1 vector system. After transformation into *E. coli* strain DH5α, the plasmids were recovered, and the cloned regions were sequenced and analyzed using MEME software.[2]

In Vitro Transcription—Supercoiled plasmid was used for *in vitro* transcription and primer extension reactions according to Lazarus and Travers (31). The mRNA obtained after *in vitro* transcription was divided into equal parts and used for primer extension by avian myeloblastosis virus reverse transcriptase (Promega) with radioactively end-labeled primers celZ1 for *celZ* mRNA and bla3B4 (5′-CAGGAAG-GCAAAATGCCGC-3′) for the *bla* transcript. The extension with primers celZ1 and bla3B4 yields 151- and 100-bp fragments, respectively. The amount of the *celZ* transcript produced was quantified and normalized to that of *bla*.

Potassium Permanganate Reactivity Assay—The reactions for potassium permanganate reactivity assays were performed with supercoiled templates. The reactions were performed similarly to those used for *in vitro* transcription, with minor modifications: plasmid DNA (500 ng) and proteins, as indicated, were incubated in 50 μl of a buffer containing 10 mM Tris-HCl, pH 7.5, 150 mM KCl, 0.4 mM dithiothreitol, and 0.1% (v/v) Nonidet P-40 (Roche Applied Science). After incubation at 30 °C for 15 min, 0.1 volume of 100 mM potassium permanganate solution was added for 15 s to the reaction mixtures containing DNA and proteins. The reactions were stopped by the addition of 0.1 volume of 14 M β-mercaptoethanol, 40 μg of glycogen (Roche Applied Science) and sodium acetate to 0.3 M, precipitated with 3 volumes of ice-cold

[1] The abbreviations used are: SELEX, systematic evolution of ligands by an exponential enrichment; RNAP, RNA polymerase.

[2] Multiple EM for Motif Elicitation (MEME) software is available on the World Wide Web at meme.sdsc.edu/meme/website/intro.html.

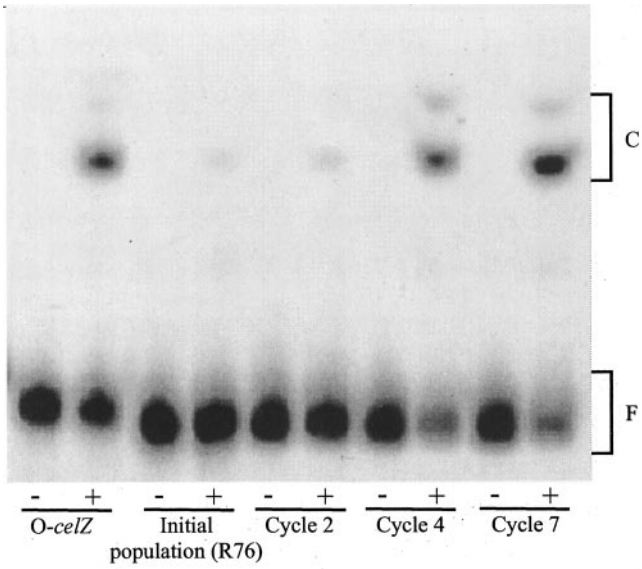

FIG. 1. **Band-shift analysis used to monitor the progress of enrichment for PecS-binding sites from random-sequence oligonucleotides.** The concentration of PecS used was 7 nM; the control probe O-celZ and the cycle of the selection of the PecS-binding sites from the random oligonucleotides R76 are indicated.

ethanol, and washed twice with 70% ethanol. The reaction products were solubilized in water and used as a template for five cycles of amplification by Taq polymerase with 5′-radio-labelled celZ1 to reveal the modified bases. The amplification products were analyzed on 6% sequencing gels.

RESULTS

Selection of the PecS-binding Site from a Pool of Random DNA Sequences—Traditional *in vitro* methods for identifying protein binding sites, such as DNase I footprinting or missing contact experiments, failed to reveal a DNA-binding consensus for PecS (22, 23, 25–27). Therefore, a SELEX strategy for selecting targets from random DNA sequences was adopted. The oligonucleotides used for selection (R76) carried constant flanking sequences for PCR, whereas the central 26 nucleotides were randomized. The enrichment of PecS-binding sites was achieved by a combination of band-shift assays and PCR amplifications. O-celZ is an 80-base pair oligonucleotide having the known high-affinity PecS-binding site of *celZ* as the central 30-base pair (26). O-celZ was used as a control to monitor the degree of enrichment at the different steps of selection. At the PecS concentration used (7 nM), only a very weak complex was observed with R76 at the beginning of the selection, whereas at least 25% of the O-celZ probe was shifted (Fig. 1). The selection-amplification cycle was repeated until no significant enrichment was observed from one step to another. This was achieved between cycles 7 and 8, wherein 7 nM of PecS caused at least 55% of the total DNA probe to be in a complex (Fig. 1). At this stage, it is supposed that a fairly pure population of high-affinity sites is selected. The DNA fragments recovered from the PecS-DNA complexes obtained after seven cycles of selection were cloned into the pCR 2.1 plasmid. Sequencing revealed 21 unique DNA fragments out of a total of 30 recovered (Fig. 2). Band-shift assays were performed with the 21 retained DNA sequences to determine their relative affinities for PecS. Protein was in excess over DNA in these experiments, and the apparent dissociation constant (K_d) was taken as the concentration of PecS that drove half of the DNA into a complex. The K_ds ranged from values similar to that of the *celZ* operator (10 nM) to that of the *pecS* operator (2 nM, the strongest natural site yet identified).

As the relative affinity of the 21 isolates varied in a 4-fold range, it was concluded that the selected DNA fragments contained PecS-binding sites. Analysis of the random sequence of the 21 selected sites was performed with the MEME software to identify a consensus motif. Based upon a matrix analysis, this software identifies conserved motifs among DNA sequences (32). The results of this computer analysis were refined by taking into account the invariant nucleotides located next to the 26 variable bases. This approach allowed for the identification of a palindromic-like consensus sequence of 23 bases: $(C_{-11}G_{-10}A_{-9}N_{-8}W_{-7}T_{-6}C_{-5}G_{-4}T_{-3}A_{-2})T_{-1}A_0T_1$ $(T_2A_3C_4G_5A_6N_7N_8N_9C_{10}G_{11})$ (Fig. 2). This consensus is characterized by the presence at both ends of C and G residues, as well as by two inverted sequences, $T_{-6}C_{-5}G_{-4}T_{-3}A_{-2}$ and $T_2A_3C_4G_5A_6$, located in the central part. Within this consensus, the four bases, G_{-4}, A_{-2}, T_2, and C_4, displaying the highest conservation rate (present in more than 90% of the selected sequences) could play a key role in the interaction with PecS. However, the consensus defined therein still tolerates an important variability, especially at positions −8, 7, 8, and 9.

As a general rule, the PecS regulator displays higher affinities for the operators which have closer similarity with the defined consensus (Fig. 2). Two sequences, RC23 (5′-CGACTTCGTATATTACGACGTCG-3′), which has the most conserved nucleotides at the different positions, and RC13, which contains the central part of the consensus (−6 to 6) (Table I), were designed to validate the deduced consensus. Titration experiments performed on these two oligonucleotides revealed that PecS displays for RC23 a K_d corresponding to the mean value observed for the majority of the 21 selected sites (5 nM), whereas the affinity measured with RC13 (K_d of 23 nM) is 4.5-fold lower than that for RC23 (Fig. 3). These results confirm that (*i*) the consensus defined indeed corresponds to the PecS-binding site, (*ii*) the most highly conserved central part of the consensus is sufficient to have a specific interaction with PecS, and (*iii*) the bases that are relatively degenerated, located at both sides of the inverted repeats, contribute to the PecS affinity for its sites.

We also constructed mutant operators in which the entire left (−11 to −1) or right (+1 to +11) half of the consensus was deleted. PecS did not bind significantly with these two oligonucleotides in the band-shift assay (data not shown), suggesting that the palindromic structure is required for the PecS dimer binding.

Consensus Base Pairs Required for High-affinity PecS Binding—To assess the contribution of the highly conserved bases G_{-4}, A_{-2}, T_2, and C_4 to the promoter activity, we synthesized various derivatives of the oligonucleotide RC23 containing one or two changes at the positions mentioned (Fig. 4). The DNA-binding properties of the PecS protein were examined first on single-mutant oligonucleotides that carried G_{-4}/A, A_{-2}/C, T_2/A, and C_4/T. Figs. 3 and 4 show that the G_{-4}/A mutant exhibited a decreased affinity of 2.5-fold for PecS, compared with that of the RC23 wild-type fragment, whereas the A_{-2}/C, T_2/A, and C_4/T substitutions caused a still more severe binding defect (between 9- and 12-fold decrease of PecS affinity) (Figs. 3 and 4). In addition, a substitution was introduced at position −1 (T_{-1}/A) to convert the central part of the consensus into a perfect palindrome and at position 0 (A_0/C) to evaluate the importance of the base at the central position. No significant difference was observed with these two mutated oligonucleotides (data not shown). Thus it appears that the four highly conserved bases, and particularly A_{-2}, T_2, and C_4, are required for efficient binding of PecS to DNA. The fact that the S1 sequence selected during the SELEX procedure, which displays a T base at position −4, shows the lowest binding capacity for PecS is consistent with this assertion.

Next, we used individual mutants containing two changes, one in each half of the consensus. Binding of PecS to the

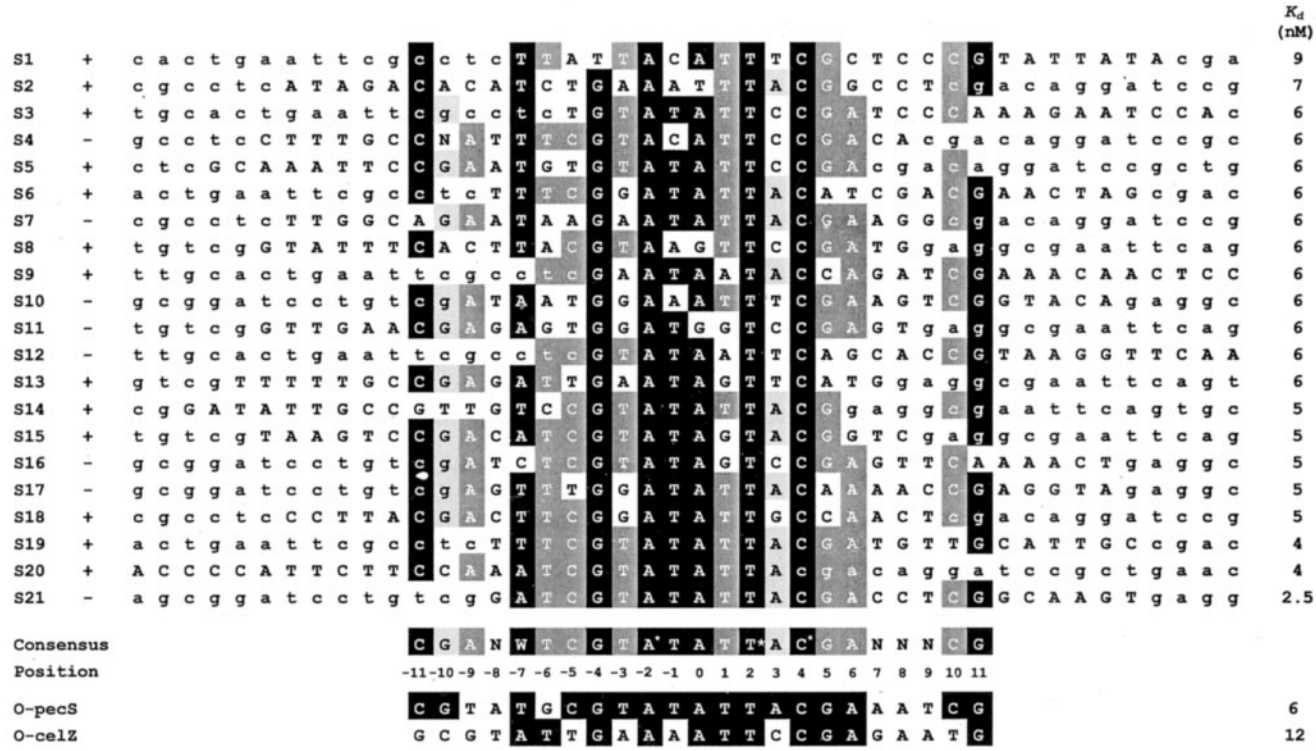

FIG. 2. **Alignment of sequences from 21 PecS-binding sites.** The alignment was carried out with MEME software. The plus and minus signs indicate the orientation of the sequence selected by the software for the alignment and correspond to the top and the bottom strands of DNA, respectively. The nucleotides localized in the central randomized part are indicated by *capital letters*; *lowercase letters* correspond to the constant flanking sequences. *Black boxes*, nucleotides displaying a conservation rate higher than 75% (among the 21 sequences); *dark gray*, conservation rates between 75–50%; *light gray boxes*, conservation rates between 50–40%. *, nucleotides conserved in all of the sequences. The deduced consensus from the alignment is indicated by the same shading. *Bottom*, nucleotides of the consensus conserved in O-pecS and O-celZ are indicated by *black boxes*. The affinity of PecS for the different binding sites is indicated on the *right*.

TABLE I
Summary of alignment of selected PecS binding site

The color code is the same as for Fig. 2.

Theoretical consensus	C	G	A	N	W	T	C	G	T	A*	T	A	T	T*	A	C*	G	A	N	N	N	C	G
RC23	C	G	A	C	T	T	C	G	T	A	T	A	T	T	A	C	G	A	C	G	T	C	G
RC13						T	C	G	T	A	T	A	T	T	A	C	G	A					
Position	-11	-10	-9	-8	-7	-6	-5	-4	-3	-2	-1	0	1	2	3	4	5	6	7	8	9	10	11
% of A	5	9,5	52.5	19	28.5	14,5	9.5	5	19	100	14	86	9.5	0	47.5	0	19	66.5	24	24	14	14	24
% of C	76	24	24	28.5	14.5	14.5	57	0	0	0	9	0	0	0	28,5	100	9.5	5	33	28,5	24	67	0
% of G	5	47,5	14	24	0	9	0	95	24	0	0	9.5	19	0	5	0	71.5	19	19	38	28,5	14	76
% of T	14	14	9,5	28.5	57	62	33.5	4,5	57	0	77	4,5	71.5	100	19	0	0	9.5	24	9.5	33.5	5	0

mutant operators in band-shift assays revealed severe reductions in affinity for two of the mutants (G_{-4}/A + T_2/A and A_{-2}/C + C_4/T, showing a 16- and a 23-fold decrease in PecS affinity, respectively) and a quasi-total impairment in the binding of PecS for two of the mutants (A_{-2}/C + T_2/A and G_{-4}/A + C_4/T) (Figs. 3 and 4). These data reveal that the modification of two bases located symmetrically in relation to the center (−4 and +4 or −2 and +2) affect more strongly the binding of PecS than does any other combination. Indeed, whereas each single T_2/A and C_4/T mutant similarly affects the PecS binding, the double A_{-2}/C+T_2/A mutant is more affected than the double A_{-2}/C+C_4/T mutant. Similarly, a single G_{-4}/A conversion leads to a less pronounced effect upon the PecS binding than does A_{-2}/C, but the double-mutant G_{-4}/A+C_4/T has a lower affinity for PecS than does the A_{-2}/C+C_4/T mutant.

The PecS Consensus Is Present in the Regulatory Regions of the Target Genes—By using *in vitro* DNase I footprinting and missing contact experiments, the presence and position of PecS-binding sites has been identified on various controlled genes: *celZ*, *pecS*, *pelD*, *pehX*, *pehV*, *pehW*, and *outC* (22, 23, 25, 26). Sequences displaying significant homology with the defined consensus were identified in each of the regions protected by PecS in DNase I footprinting experiments on these target genes (Fig. 5). Of particular interest is that PecS globally displays the strongest affinity for the natural operators (*pecS* and *celZ*) that contain a sequence showing the highest conser-

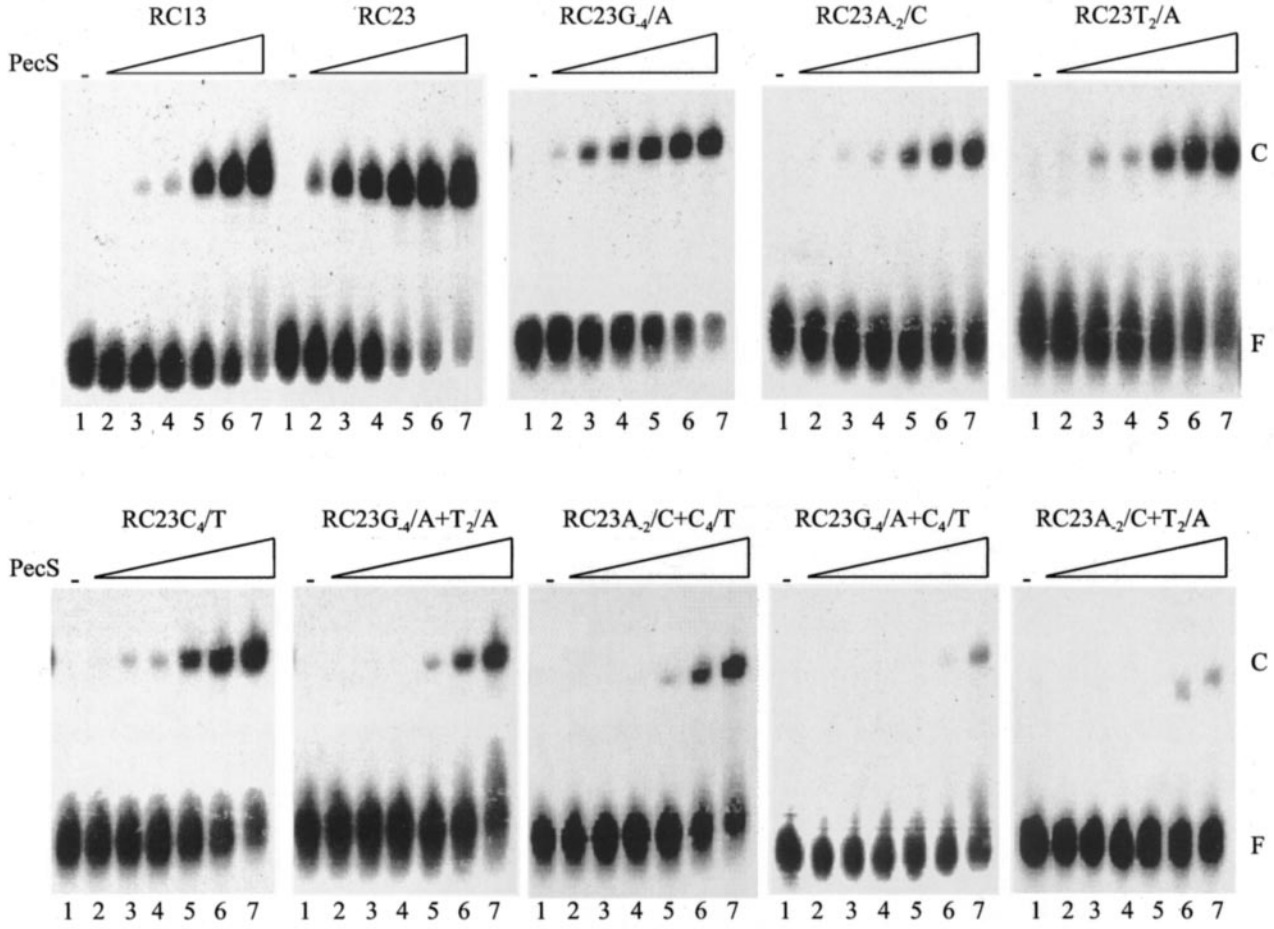

FIG. 3. **Band-shift assay for interaction of PecS with the DNA consensus sequence RC23 and its derivatives.** *Lane 1*, no protein; *lanes 2–7*, DNA with 1, 3, 9, 30, 75, and 150 nM PecS, respectively. The position of free DNA (*F*) and the PecS-DNA complexes (*C*) are indicated. Substitutions in RC23 are indicated at the *tops* of each row.

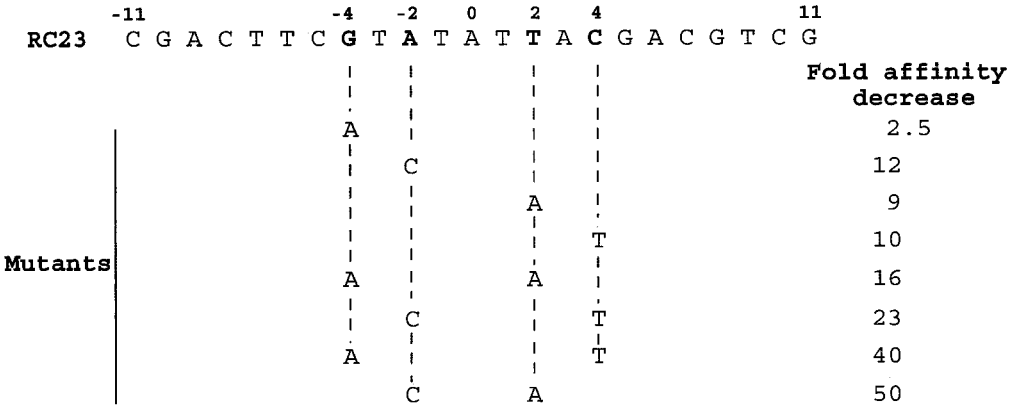

FIG. 4. **Dissection of the PecS DNA-binding consensus RC23**. The substituted bases are indicated in *bold*; relative half-maximal bindings (K_d), compared with the wild-type RC23 oligonucleotide, are shown at the *right*.

vation with the defined consensus (Fig. 5). For some operators, including *pelD*, *pehX*, *pehV*, *pehW*, and *outC*, the presence of two or several operators could compensate for the relatively high degree of degeneration of the consensus and confer an improved affinity for PecS. Alternatively, the conservation of the four bases (G_{-4}, A_{-2}, T_2, and C_4) important for the PecS binding may compensate for a relatively high global degree of degeneration in the consensus. The hypothesis of an increased affinity of the operators conferred by several binding sites was challenged by performing a PecS affinity comparison between the O-celZ or O-pecS high-affinity site-containing oligonucleotides and the *celZ* (PcelZ) and *pecS* (PpecS) natural operators. Indeed, a second degenerated consensus was identified in the low-affinity PecS-binding site on PpecS, in addition to the well conserved one (Fig. 6). A 3-fold higher PecS affinity was observed for PpecS (K_d = 2 nM) in comparison with O-pecS (K_d = 6 nM) (data not shown). Moreover, interactions of PecS with operators containing either the PpecS high-affinity site ($PpecS_H$, −183 to −46) or its low affinity site ($PpecS_L$, −48 to +166) showed that PecS displays a similar affinity for both $PpecS_H$ and O-pecS (K_d = 5 and 6 nM, respectively) but a lower affinity (K_d = 45 nM) for $PpecS_L$ (Fig. 6).

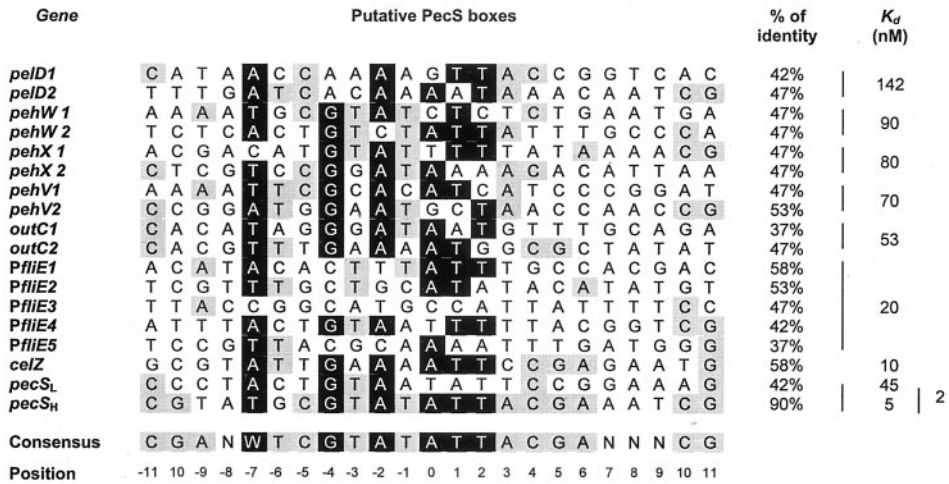

FIG. 5. **Alignment of the PecS-binding sites identified on the target genes.** The nucleotides of the defined consensus conserved in the binding sites are indicated by *shaded boxes*. *Black boxes* correspond to nucleotides present in more than 50% of the sequences; *gray boxes* indicate nucleotides with a conservation rate lower than 50%. The global percentage of the defined consensus base conservation in the sequences and the affinity of PecS for the different operators are indicated at the *right*. The different apparent K_d mentioned here were determined in the course of this work by using similar experimental conditions in the presence of the same batch of PecS and identical concentrations of the different DNA fragments.

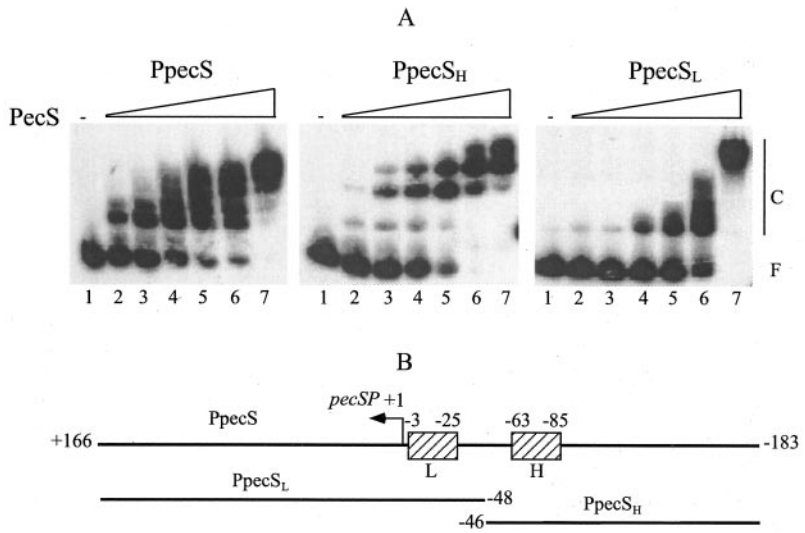

FIG. 6. **Dissection of the *pecS* gene operator.** *A*, gel-shift assay of PecS binding to the *pecS* operator PpecS and its derivatives PpecSH and PpecSL containing the high-affinity and low-affinity PecS-binding sites, respectively. *Lane 1*, no protein; *lanes 2–7*, DNA with 0.5, 1, 2, 10, 75, and 150 nM PecS, respectively. The position of free DNA (*F*) and the PecS-DNA complexes (*C*) are indicated. *B*, schematic representation of the *pecS* promoter regions, indicating the positions of the promoter elements and regulatory sites as well as the PpecS, PpecSH, and PpecSL probes; the limits of the probes are indicated with respect to the transcription initiation site of the *pecS* gene.

The fact that at a relatively high PecS concentration, several complexes appeared with the three *pecS* probes (four for PpecS and two for PpecSH and PpecSL) suggests the existence of additional degenerated PecS-binding sites on these probes (Fig. 6). The role of these putative additional PecS-binding sites was not further investigated. In the case of *celZ*, a similar PecS affinity was obtained for PcelZ and O-celZ (K_d = 10 and 12 nM, respectively), confirming that PcelZ has no additional specific PecS-binding site. Taken together, these results suggest that (*i*) PecS regulates the transcription of its target genes by binding to a specific consensus site, (*ii*) the degree of the conservation of the binding site(s) sequence *versus* that of the defined consensus determines the affinity for PecS, and (*iii*) the presence of several adjacent binding sites on the same operator increases the affinity of PecS.

Detection of a PecS-binding Site in the fliE-fliF Intergenic Region—To identify novel members of the PecS regulon in *E. chrysanthemi*, we performed a search for candidate PecS-binding sites in the complete genome of this bacteria.[3] Scanning of the *E. chrysanthemi* genome sequence with the defined consensus, using the Genome Explorer program (33), allowed us to identify a set of genes with candidate PecS-binding sites in upstream regions. Among them, we found a strong PecS consensus site (58% of identity with the defined consensus) and four other sequences displaying significant identity (53–42%), with the PecS consensus in the common regulatory region of the divergently transcribed *fliE* and *fliFGHIJKLMNOPQR* genes (Fig. 7). The most highly conserved sequence (58% of identity), designated as PfliE1, was located −110 to −88 nucleotides upstream of the translation initiation codon of *fliE*. The proteins encoded by *fliE* and *fliFGHIJKLMNOPQR* operons are involved in the biogenesis of the flagellar hook-basal body complex, which forms a flagellum export channel anchored within the bacterial membrane (34). Interestingly, the flagellum has been associated with a bacterial virulence factor because a perturbation of its synthesis results in a reduction of the pathogenic power of both animal and plant pathogenic bacteria (35, 36).

The binding of PecS to the *fliE-fliFGHIJKLMNOPQR* intergenic region was first measured by band-shift assays. Fig. 7*A* reveals that PecS could interact specifically with PfliE (−313 to +48 *versus* the translation initiation codon ATG) and that, as the concentration of PecS increased, at least five PecS-PfliE

[3] Available on the World Wide Web at tigr.org or ahabs.wisc.edu/~pernalab/.

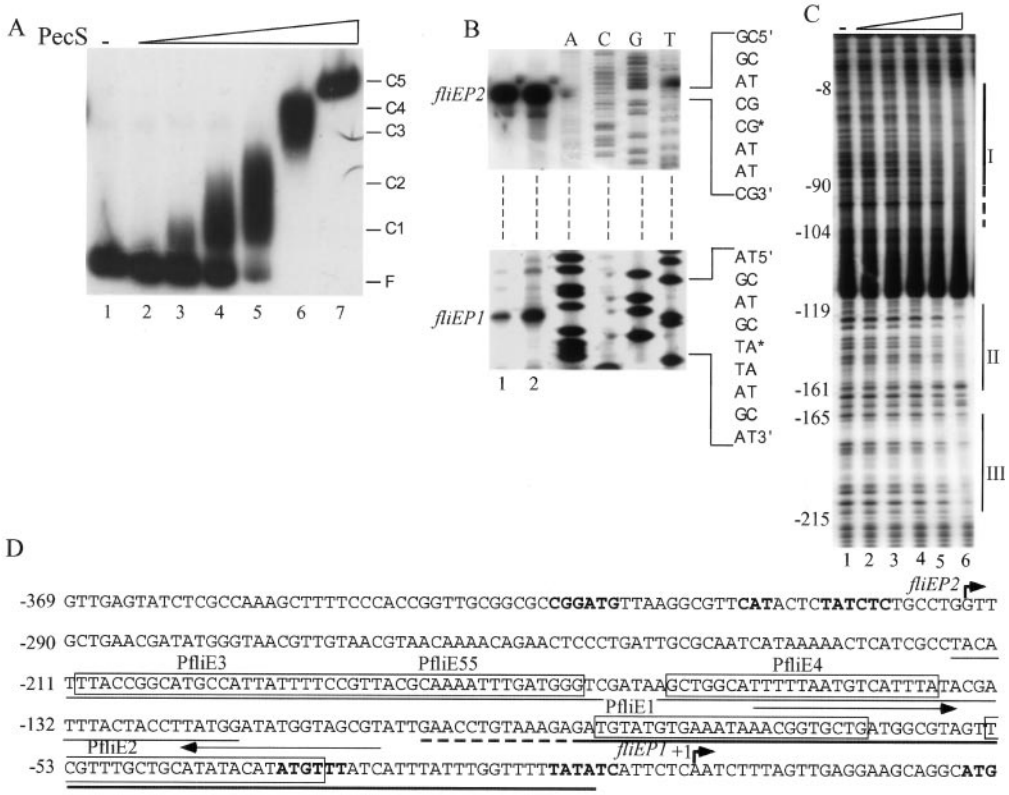

FIG. 7. **Effect of a *pecS* mutation on the *fliE* gene expression and analysis of PecS binding on the *fliE* promoter regions.** *A*, gel-shift assay. *Lane 1*, no protein; *lanes 2–7*, DNA with 3, 10, 30, 75, 250, and 500 nM PecS, respectively. The position of free DNA (*F*) and the PecS-DNA complexes (*C*) are indicated. *B*, identification of the *E. chrysanthemi fliE* transcription start sites. *Lanes 1* and *2*, reactions performed with 10 μg of RNA extracted from the parental strain A350 and its *pecS* derivative A1524, respectively. DNA sequencing ladders were generated with the same primer (*lanes A*, *C*, *G*, and *T*). The nucleotide sequences of both the coding and noncoding strands are shown on the *right*. *, the positions of the specific transcription initiation sites (at the *right*). *C,* DNase I footprinting analysis on the top strand of the promoter regions. *Lane 1*, no protein; *lanes 2–6*, DNA with 10, 30, 75, 125, and 250 nM PecS, respectively; high- and low-affinity PecS-binding sites are indicated by *bold* and *standard lines*, respectively; *dashed bold lines* correspond to the extension of the PecS high-affinity binding observed at 250 nM PecS. The sequences are numbered with respect to the transcriptional start site *fliEP1*. *D*, sequence of the *fliE* promoter. The regions protected by PecS are indicated as in *B*. The start points of transcription are shown by *arrows*, and the sequences PfliE1, PfliE2, PfliE3, PfliE4, and PfliE5, showing significant similarity with the PecS DNA-binding consensus, are *boxed*; the overlapping bases (*TCC*) of PfliE3 and PfliE5 are in *italics*. The *convergent arrows* indicate sequences showing similarity with the flagellar gene activator FlhDC-binding site (42); the potential RNA polymerase binding elements (−10 and −35 hexamers) for *fliEP1* and *fliEP2*, as well as the translation initiation codons (ATG for *fliE* and CAT for *fliF*), are in *bold characters*.

complexes could be discerned. The apparent K_d = 20 nM. These observations are consistent with the computer analysis predicting several PecS-binding sites in this DNA segment. These findings, therefore, suggest that PecS is capable of regulating the expression of the *fliE* and *fliFGHIJKLMNOPQR* operons. To confirm this assertion, primer extension analysis with RNA extracted from the *E. chrysanthemi* parental strain and its *pecS* derivative were conducted on *fliE*. Two transcription initiation sites were identified in the 5′-upstream region of this gene with both FliEpext and PfliE1R primers (*fliEP1* and *fliEP2*). Both transcripts are more highly expressed in the *pecS* context (Fig. 7*B*). The *fliEP1* position corresponds to the transcription initiation site identified for *fliE* in other enterobacteria (34). The relevance and the role of the second identified transcription initiation site (*fliEP2*) have still to be elucidated.

Finally, the regions of the DNA segment that interact with PecS were identified by DNase I footprinting analysis (Fig. 7*B*). A fully protected area, extending from −90 to −8 (Fig. 7*C*, *I*), as well as two partially protected regions (Fig. 7*C*, *II*, −215 to −165; and *III*, −161 to −119) were observed at a concentration of 125 nM of PecS in the upstream region of *fliE*. Increasing the PecS concentration up to 250 nM resulted in an extension to −104 of the 5′ limit of the region I and a full protection of the regions II and III (Fig. 7, *C* and *D*). It is important to note that region I contains the two most conserved PecS-binding sites (PfliE1 and PfliE2), and that regions II and III encompass two relatively degenerated binding sites (PfliE3 and PfliE4). In addition to these four PecS-binding sites identified by computer analysis, a fifth site, showing 37% of identity with the defined consensus, was identified in region III by further analysis. This site, which overlaps PfliE3, was named PfliE5 (Fig. 7*D*). Binding of PecS on the three regions identified by DNase I footprinting digestion would result in the inhibition of the transcription from the two *fliE* promoters. This correlates with the fact that a *pecS* mutant is hypermotile on semisolid medium, compared with the parental strain (diameter of the colony after 24 h was 4.2 cm for the *pecS* mutant *versus* 2.2 cm for the parental strain). Overall, these results indicate that PecS directly represses the *fliE* gene expression by interacting with the predicted binding sites located in the upstream region of this gene.

PecS Inhibits Transcription Initiation at the celZ Promoter—The *celZ* promoter-operator region was selected to monitor the effect of PecS on the RNA polymerase activity. Indeed, in contrast to the other strongly regulated genes such as *pecS* and *fliE*, which contain several binding sites, *celZ* contains a unique high-affinity binding site for PecS (25, 26; Fig. 8). To place the PecS-binding site at PcelZ into context it was necessary to attempt to establish the *celZ* transcription start point. Primer extension analysis with RNA from the end of exponential phase cultures (A = 0.8) of the *E. chrysanthemi* parental strain A350

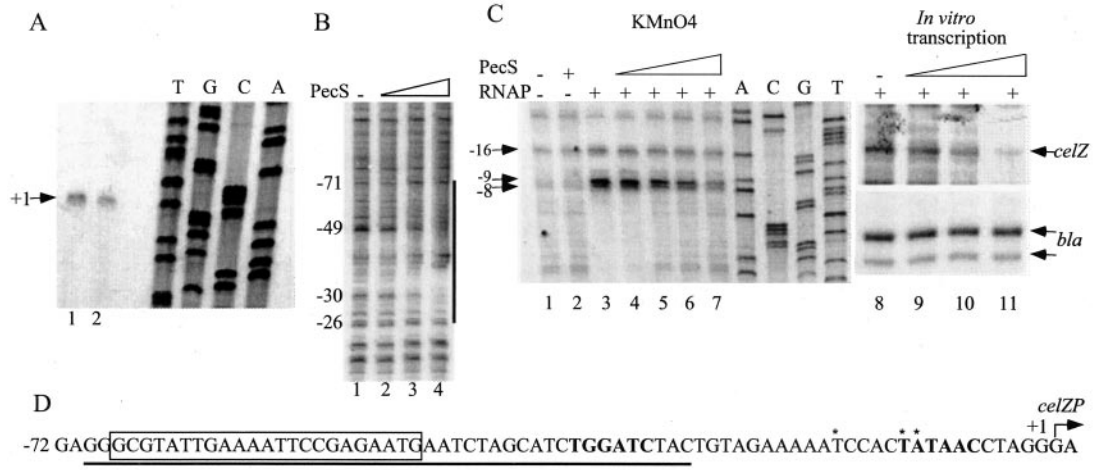

FIG. 8. **PecS prevents transcription initiation at the *celZ* promoter.** *A*, primer extension analysis of total RNA (10 μg) extracted from the *E. chrysanthemi* parental strain A350 (*lane 2*) and its *pecS* derivative (*lane 1*); the dideoxy sequencing ladder performed with the same primer on pWN2965 is shown. *B*, DNase I footprinting analysis on the top strand of the promoter regions. *Lane 1*, no protein; *lanes 2–4*, DNA with 30, 75, and 250 nM PecS, respectively. The area protected by PecS is indicated by the *black line* at the *right*. *C*, effect of PecS upon *celZ* promoter activity. The concentration of RNA polymerase was 20 nM; the concentration of PecS was 15 nM for *lanes 4* and *9*; 30 nM PecS for *lane 5*; 70 nM PecS for *lanes 6* and *10*; and 200 nM PecS for *lanes 7* and *11*. The amount of *celZ* transcript produced was quantified and normalized to that of *bla*. *D*, organization of the *celZ* promoter region. The start point of transcription is indicated by the *arrow*; the region protected by PecS in DNase I footprinting experiments is *underlined*; the sequence showing similarity with the PecS-binding site consensus is *boxed*; and the RNA polymerase binding elements (−10 and −35 hexamers) are in *bold* characters. *, bases whose modification by $KMnO_4$ is diminished in the presence of PecS.

or its *pecS* derivative revealed that *celZ* transcription was initiated at 122 bases upstream of the translation start (Fig. 8*A*). Consistent with the previous gene-fusion studies (21), a more abundant accumulation of *celZ* transcripts (5-fold) was observed in the *pecS* background than in the parental strain. Five bases further upstream, there is a potential −10 element (TATAAC) separated by 17 bases from a potential −35 element (TGGATC); thus, the *celZ* transcription start point mapped here is located in an appropriate context. It is remarkable that the region protected by PecS on PcelZ in DNase I footprinting experiments overlaps the −35 element (Fig. 8, *B* and *D*). This proximity suggests a physical basis for possible functional competition between PecS and RNA polymerase (RNAP).

The effect of PecS upon RNAP activity was investigated first by using potassium permanganate ($KMnO_4$) footprinting on supercoiled plasmid-containing PcelZ (pWN2965). $KMnO_4$ targets the pyrimidine and adenine residues in the untwisted regions of DNA and thus allows the extent of promoter opening to be measured. Upon addition of RNAP, we observed that three bases, including two at positions −9 and −8 in the predicted −10 element and another located between the −10 and −35 elements (−16), are sensitive to $KMnO_4$. Addition of PecS substantially decreased the $KMNO_4$ reactivity of these three bases (Fig. 8, *C* and *D*). From these data, we infer that binding of PecS in the *celZ* regulatory region inhibits open complex formation by RNAP. These data also indicate that the −10 and −35 elements have been correctly predicted from the transcription start site.

We next used *in vitro* transcription to directly follow the effect of PecS on the RNAP activity. For this purpose, we monitored *celZ* transcription using pWN2965 DNA with RNAP and PecS added either alone or in combination. As expected, the addition of increasing PecS concentrations gradually decreased the transcription of the *celZ* promoter (Fig. 8*C, lanes 9–11*), whereas the transcription of the reference *bla* promoter was not noticeably affected (Fig. 8*C*, *lower panel*). Thus, PecS specifically inhibits the *celZ* promoter activity *in vitro* by directly preventing transcription initiation. These results demonstrate, for the first time, repression by PecS *in vitro*.

DISCUSSION

The PecS protein of *E. chrysanthemi* belongs to the MarR family of transcriptional regulators associated with bacterial adaptation to stress (16, 37). In this respect, PecS controls the synthesis of factors required for plant defense reaction neutralization (24). Moreover, PecS regulates the synthesis of degradative exoenzymes, essentially pectinases and cellulases, which constitute the main determinant of the *E. chrysanthemi* pathogenicity (2). PecS regulates the expression of the target genes by specifically interacting with their regulatory regions. Despite specific interaction, no conserved sequence had been previously identified within the different natural binding sites of PecS (22, 25–27).

The identification of a consensus sequence for PecS is an important step in its characterization. In this study, we used the SELEX strategy and site-directed mutagenesis to identify the DNA consensus recognized by PecS ($C_{-11}G_{-10}A_{-9}N_{-8}W_{-7}T_{-6}C_{-5}G_{-4}T_{-3}A_{-2})T_{-1}A_0T_1(T_2A_3C_4G_5A_6N_7N_8N_9C_{10}G_{11}$), which defines a palindromic-like structure, the palindromic organization being required for efficient binding of PecS. The conservation rate of the nucleotides at the different positions of the consensus globally reflects their involvement in the interaction with PecS (Table I, Fig. 4). This is the answer to our first question, *i.e.* whether or not PecS binds a specific DNA sequence. The homodimeric state of PecS (25) is consistent with the recognition of a DNA target consisting of an inverted repeat in such a way that each monomer binds to a half-site. In this respect, PecS resembles MarR, MexR, and $SlyA_{ST}$ proteins, which adopt a dimeric structure to interact with a repeat composed of pentameric sub-elements separated by two bases (MarR and SlyA) or five bases (MexR) (20, 38, 39). However, the inverted repeat composed of an 11-base pair and recognized by PecS is larger than those reported for the MarR, MexR, and $SlyA_{St}$ proteins. Before our work, $SlyA_{St}$ was the only protein of the MarR family for which a consensus (TTAGCAAGCTAA) was established based upon a quantitative analysis performed on isolated sequences by SELEX experiments, as well as on the five natural sites identified in the *slyA* gene. In the case of MarR and MexR, the consensus was deduced from the alignment of only two DNase I footprinting protected areas detected

in the *marR* and *mexR* regulatory regions, respectively. However, in these three cases, only the most conserved region was selected, and the functionality of the proposed consensus was not established. In this respect, the work presented therein reveals that the relatively degenerated bases, which are located apart from the repeated pentameric motif, are also required for the efficient binding of PecS. Therefore, it can be supposed that the consensus for the $SlyA_{St}$, MexR, and MarR proteins are in fact larger than those proposed.

It is also possible that the mechanism directing the binding of PecS to its target genes is different from those proposed for the other members of this family, namely MarR, $SlyA_{St}$, and MexR. This hypothesis is supported by results concerning the crystal structure resolution of MarR, MexR, and SlyA from *Enterococcus faecalis* ($SlyA_{Ef}$), which suggest that, despite a similar global organization, these three regulators bind to DNA using distinct mechanisms (39–41). However, in the absence of crystallographic results from these proteins complexed with their DNA-binding site, this hypothesis can not be confirmed. The consensus PecS-binding site sequence ($C_{-11}G_{-10}A_{-9}N_{-8}W_{-7}T_{-6}C_{-5}G_{-4}T_{-3}A_{-2})T_{-1}A_0T_1(T_2A_3C_4G_5A_6N_7N_8N_9C_{10}G_{11}$) is also quite different from that of $SlyA_{St}$ (TTAGCAAGCTAA). The relatively important variability of the sequence of the PecS consensus-binding site suggests that it may be able to change to interact with all of its alternative binding sites. This assertion is in accordance with the high degree of flexibility of the winged-helix DNA-binding motif observed in MarR, MexR, and $SlyA_{Ef}$ proteins; this particularity is thought to favor a recognition of various DNA targets by these regulators (41). The molecular basis for the PecS binding to DNA will most likely require a detailed structural determination of the PecS protein alone and in association with its DNA-binding site. This would also shed light upon the molecular mechanism by which regulators of the MarR family recognize and bind to DNA.

The relevance of the defined PecS DNA-binding consensus was investigated first by looking at whether it is present in the previously characterized binding sites (22, 25–27). Sequences displaying significant homology with the consensus were identified in each of the natural PecS-binding sites, and an overall direct link between the conservation rate of the consensus and the affinity of PecS for the binding site was established. However, in some cases (*pelD*, *outC*, *pehX*, *pehV*, and *pehW*), a direct correlation was not strictly verified because of a cooperative effect between several less-conserved adjacent sites. This demonstrates the complexity of the mechanisms used by PecS to interact with its target genes. Moreover, in the first case, the data presented here consist of direct regulation of a great number of target genes by a member of the MarR family via a consensus.

Next, we looked to see whether the interaction of PecS with its binding site may result in a direct transcription of the expression of target genes. This question was assessed with the highly regulated *celZ* gene, which contains a unique PecS-binding site overlapping the −35 promoter element (Fig. 8; Refs. 21, 25). *In vitro* transcription and $KMnO_4$ footprinting reveal that PecS prevents RNAP access to the promoter, thereby repressing directly the *celZ* expression (Fig. 8). It is reasonable to propose that PecS represses the expression of its target genes by directly interfering with the activity of RNAP in all cases where there is an overlap or superimposition of their binding sites. Another interest in the definition of the DNA-binding consensus of the *E. chrysanthemi* multi-virulence factor regulator PecS was to look for the identification of new virulence gene(s) directly controlled by PecS. This was achieved by probing the *E. chrysanthemi* genome sequence[3] with the consensus defined here. This search allowed for the identification of the flagellar genes *fliE* and *fliFGHIJKLMNOPQR* as new PecS targets. The proteins encoded by these two transcriptional units are involved in the biosynthesis of the bacterial flagellum (34).

Flagellum-based motility has recently been recognized as a bacterial virulence factor because it enables bacteria to detect nutrients and to reach and maintain their preferred niches for colonization (36). In plant pathogens, motility seems to play a role predominantly in the early phases of infection, mediated by chemotaxis and adherence through flagella. Generally, nonflagellate mutants have a significantly reduced capacity to initiate an infection (35, 36). Thus, it is tempting to speculate that PecS regulates critical genetic determinants that are required for adaptation to the plant environment as well as for the colonization of the host tissues. Nevertheless, it is reasonable to speculate that some virulence genes directly regulated by PecS have probably not been identified in this first screen. Indeed, the possibility for PecS to specifically bind to an operator containing several relatively degenerated sites renders very difficult a search of new target genes exclusively based upon a computer investigation of the consensus. We are currently attempting to define new criteria that may incorporate this requirement.

The reported analysis of PecS represents the most detailed characterization of a regulatory mechanism of a protein of the MarR family. The definition of the PecS-binding site sequence provides solid basis for further investigation into the nature of the environmental signals perceived and the network of genes controlled by this important regulator of virulence in *E. chrysanthemi*. Such investigations will give new insights into the mechanisms used by this pathogen to evade host defenses and thus cause disease.

Acknowledgments—We thank A. Buchet, N. Hugouvieux-Cotte-Pattat, G. Condemine, and V. Shevchik for their critical opinions and V. James for reading the manuscript.

REFERENCES

1. Collmer, A., and Keen, N. (1986) *Annu. Rev. Phytopathol.* **24,** 383–409
2. Hugouvieux-Cotte-Pattat, N., Condemine, G., Nasser, W., and Reverchon, S. (1996) *Annu. Rev. Microbiol.* **50,** 213–257
3. Expert, D., and Toussaint, A. (1985) *J. Bacteriol.* **163,** 221–227
4. Bauer, D. W., Bogdave, A. J., Beer, S. V., and Collmer, A. (1994) *Mol. Plant-Microbe Interact.* **7,** 573–581
5. Condemine, G., Castillo, A., Passeri, F., and Enard, C. (1999) *Mol. Plant-Microbe Interact.* **12,** 45–52
6. Mulholland, V., Hinton, J. C. D., Sidebotham, J., Toth, I. K., Hyman, L. J., and Perombelon, M. C. M. (1994) *Mol. Microbiol.* **9,** 343–356
7. Lopez-Solanilla, E., Garcia-Olmedo, F., and Rodriguez-Palenzuela, P. (1998) *Plant Cell* **10,** 917–924
8. el Hassouni, M. E., Chambost, J. P., Expert, D., Van Gijsegem, F., and Barras, F. (199) *Proc. Natl. Acad. Sci. U. S. A.* **96,** 887–892
9. Santos, R., Franza, T., Laporte M. L., Sauvage, C., Touati, D., and Expert, D. (2001) *Mol. Plant-Microbe interact.* **14,** 758–767
10. Surgey, N., Robert-Baudouy, J., and Condemine, G. (1996) *J. Bacteriol.* **178,** 1593–1599
11. Nasser, W., Robert-Baudouy, J., and Reverchon, S. (1997) *Mol. Microbiol.* **26,** 1071–1082
12. Reverchon, S., Bouillant, M. L., Salmond, G., and Nasser, W. (1998) *Mol. Microbiol.* **29,** 1407–1418
13. Nomura, K., Nasser, W., Kawagishi, H., and Tsuyumu, S. (1998) *Proc. Natl. Acad. Sci. U. S. A.* **95,** 14034–14039
14. Nasser, W., and Reverchon, S. (2002) *Mol. Microbiol.* **43,** 733–748
15. Miller, P. F., and Sulavik, M. C. (1996) *Mol. Microbiol.* **21,** 441–448
16. Revell, P. A., and Miller, V. L. (2000) *Mol. Microbiol.* **35,** 677–685
17. Evans, K., Passador, L., Srikumar, R., Tsang, E., Nezezon, J., and Poole, K. (1998) *J. Bacteriol.* **180,** 5443–5447
18. Nagel, G., Lahrz, A., and Dersch, P. (2001) *Mol. Microbiol.* **41,** 1249–1269
19. Buchmeier, N., Bossie, S., Chen, C., Fang, F. C., Guiney, D. G., and Libby, S. (1997) *Infect. Immun.* **65,** 3725–3730
20. Stapleton, M. R., Norte, V. A., Read, R. C., and Green, J. (2002) *J. Biol. Chem.* **277,** 17630–17637
21. Reverchon, S., Nasser, W., and Robert-Baudouy, J. (1994) *Mol. Microbiol.* **11,** 1127–1139
22. Nasser, W., Schevchik, V. E., and Hugouvieux-Cotte-Pattat, N. (1999) *Mol. Microbiol.* **34,** 641–650
23. Hugouvieux-Cotte-Pattat, N., Schevchik, V. E., and Nasser, W. (2002) *J. Bacteriol.* **184,** 2664–2673
24. Reverchon, S., Rouanet, C., Expert, D., and Nasser, W. (2002) *J. Bacteriol.* **184,** 654–665

25. Praillet, T., Nasser, W., Robert-Baudouy, J., and Reverchon, S. (1996) *Mol. Microbiol.* **20,** 391–402
26. Praillet, T., Reverchon, S., and Nasser, W. (1997) *Mol. Microbiol.* **24,** 803–814
27. Rouanet, C., Noumura, K., Tsuyumu, S., and Nasser, W. (1999) *J. Bacteriol.* **181,** 5948–5957
28. Reverchon, S., Expert, D., Robert-Baudouy, J., and Nasser, W. (1997) *J. Bacteriol.* **179,** 3500–3508
29. Nasser, W., Reverchon, S., Condemine, G., and Robert-Baudouy, J. (1994) *J. Mol. Biol.* **236,** 427–440
30. Tuerk, C., and Gold, L. (1990) *Science* **249,** 505–510
31. Lazarus, L. R., and Travers, A. A. (1993) *EMBO J.* **12,** 2483–2494
32. Bailey, T. L., and Elkan, C. (1994) *Intelligent Syst. Mol. Biol.* **2,** 28–36
33. Mironov, A. A., Vinokurova, N. P., and Gelfand, M. S. (2000) *Mol. Biol.* **34,** 253–262
34. Chilcott, G. V., and Hughes, K. T. (2000) *Microbiol. Mol. Biol. Rev.* **64,** 694–708
35. Chesnokova, O., Coutinho, J. B., Khan, I. H., Mikhail, M. S., and Kado, C. I. (1997) *Mol. Microbiol.* **23,** 579–590
36. Josenhans, C., and Suerbaum, S. (2002) *Int. J. Med. Microbiol.* **291,** 605–614
37. Alekshun, M. N., and Levy, S. B. (1997) *Antimicrob. Agents Chemother.* **41,** 2067–2075
38. Martin, R. G., and Rosner, J. L. (1995) *Proc. Natl. Acad. Sci. U. S. A.* **92,** 5456–5460
39. Lim, D., Poole, K., and Strynadka, C. J. (2002) *J. Biol. Chem.* **277,** 29253–29259
40. Alekshun, M. N., Levy, S. B., Mealy, T. R., Seaton, B. A., and Head, J. F. (2001) *Nat. Struct. Biol.* **8,** 710–714
41. Wu, R. Y., Zhang, R. G., Zagnitko, O., Dementieva, I., Maltzev, N., Watson, J. D., Laskowski, R., Gornicki, P., and Joachimiak, A. (2003) *J. Biol. Chem.* **278,** 20240–20244
42. Claret, L., and Hughes, C. (2002) *J. Mol. Biol.* **321,** 185–199